Solar Energy Vol. 51, No. 6, pp. 449–456, 1993
Printed in the U.S.A.

0038–092X/93 $6.00 + .00

SOLAR IRRADIANCE ESTIMATION FROM GEOSTATIONARY SATELLITE DATA: I. STATISTICAL MODELS

M. NOIA,* C. F. RATTO, and R. FESTA
Department of Physics, University of Genoa, Italy

Abstract—The use of satellite data to estimate solar irradiance at ground level represents a valid alternative to ground measurements of solar radiation. The best known methods of estimating the solar irradiance at the earth's surface using geostationary satellite data are reviewed. The models may be classified into statistical and physical models, depending on the approach used to treat the interaction between solar radiation and atmosphere. The main hypotheses and algorithms used in four statistical models are extensively presented and discussed. The differences between these methods are pointed out. Physical models will be examined in a second paper[1]. This second paper will include various assessments regarding the performances of the described methods and summaries of comparisons between the different models.

1. INTRODUCTION

The knowledge of the solar radiation reaching the earth's surface and its geographical distribution is very important for solar energy and other applications. The availability of solar radiation data is limited by the sparsity of the existing networks. Efforts to infer insolation from conventional meteorological observations such as cloud cover, cloud type, and precipitable water are generally insufficient for producing accurate insolation estimates at all locations of interest. Consequently, the meteorological satellite appears as a practical source of data having the required information content. An alternative approach consists of spatially interpolating, using more or less sophisticated algorithms, the data measured at ground level[2–5]; the two philosophies have been fused together quite recently[6].

Earlier attempts to utilize satellite data for estimating incident solar radiation at the earth's surface are found in the works of the U.S. Department of Commerce[7], Vonder Haar[8], Vonder Haar and Ellis[9,10]. All these methods were based on the images provided by polar satellites. A major drawback of these early insolation studies was the limited temporal coverage provided by the polar orbiting meteorological satellites (only one or very few daylight images per day). This meant that cloud cover variations could not be taken into account within the framework of these early studies.

The problem of cloud cover variability was solved by using data from geostationary meteorological satellites. The data provided have high temporal resolution as these satellites are able to provide a new image of the same region every 30 minutes, with good spatial resolution ($1 \div 5$ kilometers at the subsatellite point).

In order to estimate solar irradiation incident at ground level from satellite images, two different approaches were developed.

The first approach is represented by several models, dated between 1978 and 1986, based on statistical regressions between the digital count measured by the satellite radiometer in a given area and the simultaneous solar radiation value measured at the earth's surface by a pyranometer in a station within the considered area. These are commonly called statistical models.

The second approach is represented by the models, published between 1980 and 1987, based on a radiative transfer model that explicitly describes the physical processes (i.e., scattering and absorption) operating in the earth-atmosphere system. These are usually referred to as physical models.

In this paper, we will describe the ideas and approximations on which statistical models are based, with a review of some of the main models developed, i.e., those developed by Hay and Hanson[11], Tarpley[12], Justus, Paris, and Tarpley[13], and Cano[14]. The physical models will be examined in a second paper[1].

The performances of some of these models were tested in several applications (e.g., Raphael[15], Raphael and Hay[16], Czeplak[17], and Zelenka *et al.*[18]). In these studies, the results obtained by means of satellite data were compared with ground solar radiation data provided by pyranometers. In all the models tested, the errors in the estimation of solar radiation were comparable with the errors provided by the pyranometers.

2. PHYSICAL BASIS OF ALL METHODS

The extraterrestrial solar radiation incident at the top of the atmosphere, after penetrating into it, interacts

---

* Present address: AGIP S.p.A.-Drilling and Completion, R&D Dpt., Milano, Italy.

This work is partly based on Mr. Noia's thesis. It is also intended as a contribution to Task 9 (Solar Radiation and Pyranometric Studies) of the Solar Heating and Cooling Programme of the International Energy Agency.

with molecular gases, aerosol particles, and cloud droplets. A part of this radiation is backscattered toward space, a part is absorbed, and the remainder reaches the ground. The radiation reaching the ground interacts with the earth's surface: a part of this radiation is absorbed by the ground, while the remainder is again reflected toward space. Therefore, the solar radiation emerging from the atmosphere is composed of the solar radiation backscattered by the atmosphere before reaching the ground, and by that reflected by the earth's surface back through the atmosphere, as illustrated in Fig. 1.

When considering the energy conservation in an earth-atmosphere column, we can write (see Fig. 1):

$$IE_{\downarrow} = IE_{\uparrow} + E_A + E_G \tag{1}$$

where

$IE_{\downarrow}$ represents the flux density of the downward solar radiation incident on the atmosphere;

$IE_{\uparrow}$ represents the flux density of the upward solar radiation emerging from the atmosphere and measured by the satellite;

E_A is the fraction of $IE_{\downarrow}$ absorbed by the atmosphere; and

E_G is the fraction of $IE_{\downarrow}$ absorbed by the ground.

The solar radiation absorbed by the ground can be expressed in terms of the surface albedo A and the solar irradiance at the surface IG:

$$E_G = IG(1 - A). \tag{2}$$

Hence, substituting eqn (2) in (1) and solving for IG, we obtain:

$$IG = \frac{1}{1 - A}[IE_{\downarrow} - IE_{\uparrow} - E_A]. \tag{3}$$

$IE_{\downarrow}$ depends on the sun zenith angle and on the sun-earth's distance and can be computed by means of the following equation:

$$IE_{\downarrow} = F_{cs}\left(\frac{r_o}{r}\right)^2 \cos\theta \tag{4}$$

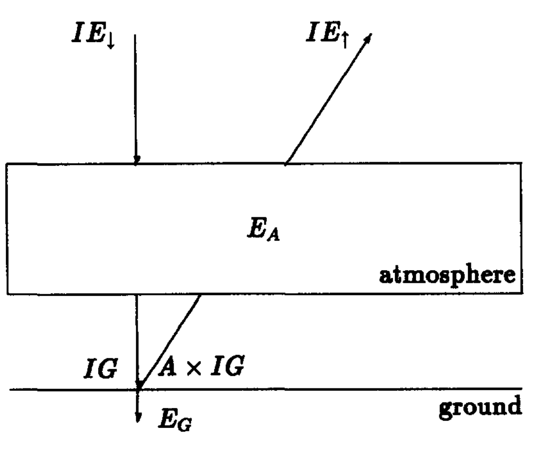

Fig. 1. Solar radiation fluxes in the atmosphere.

where

$F_{cs} \simeq 1367$ W/m^2 is the solar constant;

r_o and r are, respectively, the mean and the actual sun-earth distance; and

θ is the sun zenith angle.

Note that since radiometers on board satellites are sensitive to visible radiation in a window (e.g., 0.40 ÷ 1.10 μm for METEOSAT) narrower than the full solar radiation spectrum, some authors (e.g., Marullo *et al.*[19]) used a corrected (i.e., smaller) value of the solar constant.

If we were able to estimate E_A and know, *a priori*, the surface albedo A, eqn (3) could be used to estimate IG from the values of $IE_{\uparrow}$ measured by the satellite radiometer. Unfortunately, the problem is more complex, since it is not possible to know the surface albedo A for every point of the region studied and, on the other hand, the value of E_A is very variable and depends on the atmospheric conditions.

One of the most important factors affecting both the incoming solar radiation at the earth's surface and the solar radiation emerging from the atmosphere, is the change in the sun zenith angle and the corresponding change in the air mass through which the sun radiation travels.

The second largest cause results from the presence of clouds. The presence of water droplets and of ice particles in clouds strongly increases both the absorption and scattering of solar radiation. Changes in atmospheric water vapor or aerosol content can be considered as second-order effects on insolation.

Since changes in solar zenith angle can be calculated exactly, if we can outline cloud regions in the satellite images and evaluate their effects on solar radiation with reasonable accuracy, we might then be able to estimate insolation in both clear and cloudy conditions.

Moreover, the flux density $IE_{\uparrow}$ measured by the satellite is very sensitive to cloud cover, since clouds can be intense reflectors of visible solar radiation. As a result, the upward flux density $IE_{\uparrow}$ associated with a cloudy region is, in general, much larger than the brightness of a clear sky area (except for snow or ice covered regions) and can be used to detect the presence or absence of cloud.

In the following section we will see that some models also use the values of the infrared radiation flux reaching the satellite in order to improve the distinction between cloud cover and some types of land.

3. GENERAL DESCRIPTION OF THE METHODS

The methods used to estimate the solar irradiance at ground level, as already pointed out, may be divided into statistical and physical methods.

Statistical methods are based on one or more relationships, treated as statistical regressions, between the solar radiation measured by means of a pyranometer in a meteorological station and the simultaneous digital count value provided by the satellite for the location corresponding to the pyranometer site: this relationship is assumed valid and then used to estimate the solar irradiance at ground level for the entire region under consideration. Several independent variables enter the regression equations; these are: cosine of the sun zenith angle $\cos\theta$, which gives information on the downward extraterrestrial flux incident on the atmosphere; cloud cover index n, which describes the amount of cloud cover over the region studied; atmospheric transmittance $T(\theta) = IG/IE_\downarrow$, which takes into account the solar radiation attenuation produced by the atmospheric components; brightness B, measured by the satellite, which gives information on the upward solar radiation emerging from the atmosphere; clear-sky brightness or simply clear brightness B_0, which gives information on the ground albedo; and maximum brightness B_{max}, which gives information on the cloud albedo.

As already stated, the physical methods and their associated quantities will be examined in a second paper[1].

The main advantage (see Table 1) of the statistical methods is their simplicity and consequent operational efficiency. They use the digital count values provided by the satellites directly and do not need to convert these values into the flux density of the upward solar radiation emerging from the atmosphere. Moreover, these methods do not normally need complementary meteorological data (i.e., temperature, humidity, and precipitable water).

The main limitations of the statistical methods are the need for ground solar radiation data and the lack of generality. It must be remembered that the same regression equation coefficients, determined for the locations corresponding to the ground solar radiation data, are also used to estimate the solar radiation reaching the ground throughout the region studied. Furthermore, there is no guarantee that they would have the same values in other areas.

A difficulty common to both statistical and physical methods (but more meaningful for the first) is that the—space and time—scales of satellite images are different from those of ground-based measurements.

In particular, two problems arise when comparing the satellite data with ground solar radiation measurements. The first problem is given by errors in the localization of the pyranometer sites on the satellite images. The second problem is that satellite data are instantaneous measurements over a small solid viewing angle, while ground measurements are integrated over time (usually one hour) and a solid angle of 2π.

The solution to both problems found by researchers in this field is the use of target areas including more pixels. For instance, Tarpley[12] used target areas of 7×6 pixels ($\sim 50 \times 50$ km), centered on the intersections of 0.5° latitude and longitude lines, and used a 2° grid to calculate the clear brightness (see subsection 4.2); Gautier *et al.*[20] averaged the solar radiation estimates on a 8×8 pixel array; Justus, Paris, and Tarpley[13] considered target areas of 5×5 pixels ($\sim 40 \times 40$ km); Raphael[15] and Raphael and Hay[16] calculated the radiation on a 5×5 pixel array centered on any given station.

4. STATISTICAL METHODS

4.1 *HH model*

The simplest statistical method is that developed by Hay and Hanson[11], here referred to as the HH method. This method only uses visible satellite data. In addition, in spite of that written by us on the general features of the statistical methods, this method does require the calibration of the satellite data.

The HH model[11] was part of a study undertaken, for the Global Atmospheric Research Program Atlantic Tropical Experiment, to map the distribution of shortwave radiation incident at the sea surface, using satellite observations in the visible region of the spectrum (0.55 ÷ 0.75 μm).

The method used is based on a simple linear relationship between the visible radiance $\frac{IE_\uparrow}{IE_\downarrow}$ and the atmospheric shortwave transmittance T, where $\frac{IE_\uparrow}{IE_\downarrow}$ is the irradiance measured by the satellite sensors and normalized to the extraterrestrial irradiance $IE_\downarrow$ while T is the ratio between the irradiance at the surface IG and the extraterrestrial irradiance.

This relationship is:

$$T = a - b\frac{IE_\uparrow}{IE_\downarrow} \tag{5}$$

where a and b are the regression coefficients to be evaluated.

Note that the digital counts provided by the satellite have to be transformed into the visible radiance using calibration procedures.

Substituting eqn (4) in eqn (5), this becomes:

$$IG = TF_{cs}\left(\frac{r_0}{r}\right)^2 \cos\theta. \tag{6}$$

The values of the regression coefficients a and b determined by Hay and Hanson are:

$$a \simeq 0.79 \quad b \simeq 0.71.$$

Table 1. Advantages and disadvantages of statistical and physical methods

	Statistical	Physical
Advantages	• operational efficiency • no need for meteorological data • no need for calibration	• generality • no need for ground solar radiation data
Disadvantages	• need for ground solar radiation data • lack of generality	• need for meteorological data • need for calibration

Raphael and Hay[16](see section 6) find a better agreement with their data base using the following values of coefficients a and b:

$$a \simeq 0.788 \quad b \simeq 1.078.$$

Note that the atmospheric transmittance changes with the content of the atmosphere changes. An increase in the concentration of aerosols and dust particles, water vapor, and cloud cover, produces an increasing scattering in the atmosphere: this results in a decrease in the atmospheric transmittance and ground-measured insolation and consequently to an increased satellite-measured radiance. On the other hand, an increased absorption will reduce the radiation measured at the surface and, at the same time, the radiance measured at the satellite. Thus a decreasing relationship between atmospheric transmittance and satellite measured radiance—as shown by eqn (5)—should easily contain the variations in scattering which influence the irradiance measured at the surface, though would be less reliable when absorption is significant.

The relationship breaks down under conditions of high surface albedo (e.g., a snow- or ice-covered surface). The high albedo will increase both the brightness measured by the satellite (except under heavily overcast conditions) and the radiation measured at the surface due to the effect of multiple reflections. This would lead to a significant underestimation of the radiation at the surface, particularly under a clear sky.

4.2 *T model*

The method developed by Tarpley[12]represents part of the outcome of an experiment conducted in the summer of 1977 over the U.S. Great Plains. In this study GOES images were used.

To account for different physical processes depleting the incoming solar radiation under clear, partly cloudy, and cloudy conditions, the T model uses three different equations, according to the amount of cloud in the target, in order to calculate the hourly solar irradiation, as follows:

$$HG = a + b\cos\theta + cT + dn + e\left(\frac{B_m}{B_0}\right)^2 \quad (n \leq 0.4)$$

$$HG = a + b\cos\theta + cn\left(\frac{B_{cld}}{B_n}\right)^2 \quad (0.4 \leq n \leq 1.0)$$

$$HG = a + b\cos\theta + c\left(\frac{B_{cld}}{B_n}\right)^2 \quad (n = 1). \tag{7}$$

where

HG = hourly surface irradiation;
θ = local solar zenith angle;
n = cloud index;
B_m = mean target brightness, defined as the mean brightness of a 7 × 6 pixel array;
B_0 = clear brightness;
B_{cld} = mean cloud brightness, computed by averaging the brightness values of all the pixels in the 7 × 6 array that are brighter than a given threshold T_2;
B_n = B_0 (θ = 45°, ϕ = 105°) = normalized clear brightness; where ϕ is the azimuth angle between sun and satellite, illustrated in Fig. 2. T and θ were already defined.

To determine cloud characteristics, it is necessary to know when each pixel is cloud free. Tarpley calculated an experimental clear brightness B_0 value from the following regression:

$$B_0 = a + b\cos\theta + c\sin\theta\cos\phi + d\sin\theta\cos^2\phi. \tag{8}$$

The second term on the right hand side of eqn (8) accounts for the changing incident flux; the following two terms are introduced to account for changes in target brightness due to shadowing at the surface and anisotropic scattering.

In order to compute the clear brightness regression coefficients a, b, c, and d, more than 100 observation targets were collected by Tarpley during the 27 days prior to the test period. Mean standard deviation and the solar azimuth and zenith angles were computed for each day and for each target and then stored.

Tarpley adopted the following automatic cloud detection and elimination procedure:

- data with solar zenith angles > 85° were discarded;
- data with too large target standard deviations were discarded in order to produce a sufficiently cloud-free data set;
- a "first guess" of the coefficients of the clear brightness equation was calculated;
- data with brightness greater than that predicted, were eliminated from the data base; and
- after three cycles of the last two steps, this procedure yielded a cloud-free data set and reliable regression coefficients.

Note that targets containing features with markedly contrasting brightness, such as steep mountains, coastal areas, and great lakes, could not be accurately fitted to the regression equation.

Cloud amount in each target is determined using a two-threshold method, originally developed by Shenk and Salomonson[21]. This method classifies the pixels into three classes: clear, partly cloudy, and cloudy, sep-

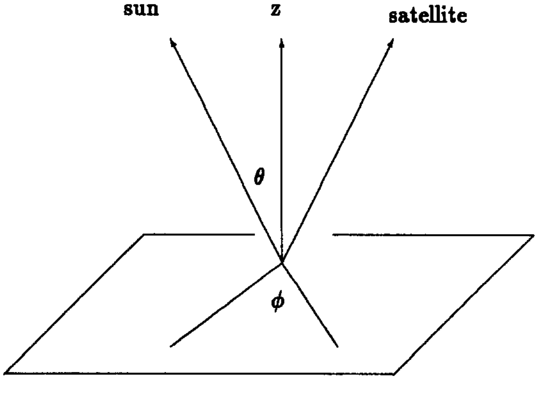

Fig. 2. Solar and satellite angles used in the clear brightness equation.

arated by two threshold values: T_1 (clear/partly cloudy threshold) and T_2 (partly cloudy/cloudy threshold), defined with respect to the clear brightness B_0.

Cloud index n relative to a target is determined from the following expression:

$$n = \frac{0.5N_2 + N_3}{N} \tag{9}$$

where N is the total number of pixels in a target area, and N_2 and N_3 are the numbers of pixels in partly cloudy and cloudy categories respectively.

Finally, Tarpley calculated the atmospheric transmittance T as the product of the visible transmission factors due, respectively, to water vapor scattering, water vapor absorption, and Rayleigh scattering, calculated as functions of the precipitable water w and of the optical air mass m, as performed by Davies *et al.*[22]and McDonald[23].

The values of the regressions coefficients a, b, c, d, and e determined by Tarpley are reported in Table 2 in kJ m^{-2}, together with the values obtained by Raphael[15]and Raphael and Hay[16]in their experiments (also see section 6).

4.3 *JPT model*

The model developed by Justus, Paris, and Tarpley[13]was part of the Agriculture and Resources Inventary Surveys through Aerospace Remote Sensing (AgRISTARS) program and was applied to produce insolation maps of the United States, Mexico, and South America. GOES images were used in the paper. The JPT model is a simplification of the T model, since it presents only one regression equation valid for all cloud conditions and does not need supplementary meteorological data such as precipitable water.

The algorithm by Tarpley, which replaces eqn (8), is represented by the following equation:

$$HG = F_0\left(\frac{r_0}{r}\right)^2 \cos\theta[a + b\cos\theta + c\cos^2\theta] + d(B_m^2 - B_0^2) \tag{10}$$

Table 2. Regression coefficients entering in eqn (7) as determined by Tarpley[12]and—in parenthesis—by Raphael and Hay[16]

Coefficients	Clear $n < 0,4$	Partly cloudy $0,4 \le n < 1,0$	Cloudy $n = 1,0$
a	−809.54 (−195.67)	−400.79 (−199.30)	−274.73 (−49.80)
b	3646.91 (3722.93)	3959.34 (4047.97)	3672.04 (2187.16)
c	1155.10 (85.98)	−319.13 (−329.30)	−314.10 (−168.80)
d	−438.90 (151.10)		
e	−266.78 (−90.86)		

Units: kJ m^{-2}.

Table 3. Regression coefficients entering in eqn (11) as proposed by Justus *et al.*[13]

a	b	c	d
0.4147	0.7165	−0.3909	−1.630

a, b, and c are dimensionless; d is in kJ m^{-2}.

where
F_0 is the hourly total value for the solar constant;
B_m is the observed mean target; and
B_0 is the clear brightness, defined below.

The last term on the right hand side of eqn (10) is the cloud correction term. It was chosen by the authors of the model as being proportional to the difference between the square of the observed radiance and the square of the clear-sky radiance, in that they used satellite data from GOES, the nominal calibration of which has radiances proportional to the square of brightness counts.

To account for variations in the directional reflectance of the earth-atmosphere system due to variations in earth-location position, viewing angle, and solar illumination angle, Justus *et al.*[13]determine values of the clear brightness for each satellite viewing time and for each of the target areas using the following procedure ("minimum brightness technique").

The authors assume that, for a particular time of day and for each target area, a brightness under clear sky conditions B_0' and the corresponding observed mean target brightness B_m are known (see subsection 4.2). Two thresholds $B_{\min}$ and $B_{\max}$ are predetermined, indicating a likely presence of clouds at the time of observation ($B_m > B_{\max}$) or insufficient scene illumination for insolation estimates ($B_m < B_{\min}$).

A new clear brightness value is determined by the relationships:

$$
\begin{aligned}
B_0 &= B_0' && \text{if } B_m \ge B_{\max} \\
B_0 &= w_1 B_0' + (1 - w_1)B_m && \text{if } B_0' < B_m < B_{\max} \\
B_0 &= B_m && \text{if } B_0' - 2 < B_m \le B_0' \\
B_0 &= w_2 B_0' + (1 - w_2)B_m && \text{if } B_{\min} \le B_m \le B_0' - 2 \\
B_0 &= B_0' && \text{if } B_m < B_{\min}
\end{aligned}
$$

where the weights w_1 and w_2 can have values between 0 and 1, and $B_{\min}$ and $B_{\max}$ are the already defined predetermined threshold values. The values of w_1 and w_2, empirically determined by Justus, Paris, and Tarpley[13], are 0.99 and 0.90, respectively.

The first equation (likely presence of clouds at the time of observation) and the fifth equation (insufficient scene illumination for solar radiation estimates) leave the clear brightness unchanged; the second equation allows a small increase in clear brightness in order to take into account seasonal variations in surface reflectance or solar illumination angle; the third equation replaces the current clear brightness value with any lower count (i.e., clearer sky) values encountered; the fourth equation is an attempt to suppress spurious effects on B_0 values which occasionally occur in the satellite images.

The values of the regression coefficients a, b, c, and d given by the authors are reported in Table 3.

4.4 *C method*

The method developed by Cano[24]and Cano *et al.*[14], subsequently slightly modified by Diabaté *et al.*[25,27]and Moussu *et al.*[26], represents the basis for the HELIOSAT project of Ecole Nationale Superioure des Mines de Paris, Sophia-Antipolis (France). This approach was developed to treat METEOSAT images in the visible channel.

The basic idea of the C method is that the amount of cloud cover over a given area statistically determines the global radiation for that area. Thus the processing is divided in the following steps:

- a map of the reference ground albedo is constructed and updated daily, giving information on the clear-sky planetary albedo for every pixel;
- a cloud cover index map is drawn from the comparison of the current satellite image and the reference albedo map;
- the atmospheric transmittance factors are computed using pyranometric data, and a statistical linear regression is then performed between these factors and the cloud cover index at the same location; and
- finally the atmospheric transmittance factors, computed for every pixel using an interpolation technique, are used to construct the global radiation map.

The parameter playing a central role in the Cano model is the total atmospheric transmission factor T^t, defined as:

$$T^t = \frac{IG}{IE_\downarrow} \simeq \frac{HG}{HE_\downarrow} \tag{11}$$

where IG and HG are the global irradiance and the global hourly irradiation on the ground and $IE_\downarrow$ and $HE_\downarrow$ are the irradiance and the hourly irradiation at the top of the atmosphere, respectively.

On the basis of some realistic hypothesis, Cano *et al.*[14]assume that a linear relationship exists between T^t at point (i, j) for a given time t and a suitably defined cloud cover index $n^t(i, j)$ at the same point and same time:

$$T^t(i,j) = a(i,j)n^t(i,j) + b(i,j) \tag{12}$$

where $a(i,j)$ and $b(i,j)$ are the regression coefficients.

The regression coefficients can be determined by comparing the transmission factors deduced from the solar radiation data measured at ground level with the corresponding cloud cover index derived from satellite images. Once these coefficients are known at ground stations, methods of interpolation may be applied in order to define the complete field of coefficients for the area studied.

The cloud cover index is given by the formula:

$$n^t(i,j) = \frac{\rho^t(i,j) - \rho_0(i,j)}{\rho_c - \rho_0(i,j)} \tag{13}$$

where $\rho^t(i,j)$ is the apparent ground albedo at a given point, $\rho_0(i,j)$ is the reference ground albedo at the same point, and ρ_c is the average albedo of the cloud tops. Note that the values assumed by n^t range from 0 to 1: thus it can be interpreted as the percentage of the cloud cover per pixel.

The reference ground albedo for clear-sky conditions ρ_0 is calculated following the Bourges model[28], which describes the solar irradiance received by the satellite in clear-sky conditions $IE_\uparrow$ either as:

$$IE_\uparrow = 0.7\rho_0 IE_\downarrow(\sin\theta)^{1.15} \tag{14}$$

or as[26]:

$$IE_\uparrow = 0.7\rho_0 IE_\downarrow(\sin\theta \sin\theta_s)^{1.15} \tag{15}$$

where $IE_\downarrow$ is the extraterrestrial irradiance incident on the top of the atmosphere, θ is the solar zenith angle, and θ_s represents the satellite zenith angle.

The reference albedo of the ground is then evaluated at each pixel following a recursive procedure, minimizing the variance of the difference between the measured radiances and the radiances resulting from the clear-sky model, the cloudy cases being eliminated at each step.

Cloud detection can be performed from the difference between the cloud induced (higher) response and the corresponding (lower) response relative to the ground under a clear-sky†.

The inverse of the algorithm used to draw the reference map of the ground albedo is applied to the construction of a cloudy-only image obtained retaining only the cloudy cases: this procedure provides an estimation of the average albedo of the cloud top ρ_c.

In the case of snow or ice covered areas and desert areas, Cano[24]and Cano *et al.*[14]proposed a similar expression using the radiance $R^t(i,j)$ measured by the satellites in the thermal infrared spectral band instead of the corresponding already defined albedoes.

5. COMPARISON BETWEEN MODELS

All the models described were tested, both by their respective authors and by other scientists, with experimental data.

Few studies compared different models using a single homogeneous data set. A detailed assessment of three models (HH, T, and GDM, with our notations; see also[1]) has been performed by Raphael[15]and Raphael and Hay[16].

Ground truth radiation data for these studies come from a 12-station pyranometric network spanning a 45 × 70 km section of British Columbia, Canada. A total of 21 days were selected to include variable sky cover conditions in all seasons. Only the visible data, in the 0.55 ÷ 0.75 μm region, measured by the GOES-

† The iterative procedure usually converges to the mean ground albedo value: important exceptions are snow, some desert surfaces, and clouds stationary in the examined time-series.

2 satellite were used: these were in the form of counts on a 8-bit scale ranging from 0 to 255 with a resolution of four counts. The resolution of the satellite was of the order of 1.4 km^2, but the accuracy of the earth location of the satellite imagery (the accurate aligning of points on the image to the same points on the earth's surface) was within ± 2 pixels.

Czeplak, Noia, and Ratto[17] compared the T and the MR models (see also[1]). Ground truth radiation data for this study came from a 29-station pyranometric network of West-Germany.

5.1 *HH model*

The HH model[11] was originally developed and tested using data from the tropical Atlantic: the estimates obtained of the measured radiation were within ± 22% on a hourly basis, improving to ± 8% on a daily basis.

Raphael[15] and Raphael and Hay[16] pointed out the inability of the regression coefficients, developed for the tropical Atlantic, to describe the conditions at midlatitude locations, mainly under the partly cloudy and overcast conditions, due to the generally different cloud regimes. The HH model, with coefficients revised by Raphael, underestimated the measured radiation on the partly cloudy day considered, though without significant bias for the clear and the overcast day.

5.2 *T model*

Estimates based on the T model were within 10% of the mean measured daily radiation.

In the application by Raphael[15] and Raphael and Hay[16], this model was shown to systematically underestimate the measured radiation for the chosen partly cloudy and clear days. On the other hand, overestimation under overcast conditions is attributed to the inadequate handling of cloud absorption. Increases in the rms error from clear through to overcast conditions were pointed out.

After their revision [regression coefficients entering in eqn (8)], the bias for clear sky conditions was reduced on average to zero, with a concomitant decrease in the rms error to a value near ± 5%. This result is—in this particular experiment—better than those obtained with HH and GDM models (see[1]).

Little improvement was obtained for a partly cloudy day and overcast conditions: the value given to the threshold separating partly cloudy from overcast conditions is considered very critical.

5.3 *JPT model*

The authors of this method claim, in their paper, that their estimates are within ± 16.2% on an hourly basis, and within ± 9.5% on a daily basis.

5.4 *C method*

The results obtained by Cano *et al.*[14] were affected by a standard error of about ± 30 J m^{-2} relating to global hourly values.

6. CONCLUSIONS

The main hypotheses and algorithms used in four statistical methods for estimating the solar irradiance at ground level using satellite data have been presented and discussed.

The methods range from a simple empirical linear regression between ground global radiance and satellite visible radiance (HH model); regressions which take into account the status of the sky (cloudy, partly cloudy, clear) through a parametrization of the cloud index and atmospheric transmittance (T model); or through a suitable piece by piece evaluation of the clear sky brightness based on predetermined threshold values (JPT model); to estimates based on the calculation of the cloud cover index using a reference albedo and an average albedo at the cloud top (C model).

All these models produce estimates of the ground global irradiations to more or less within 10% of the measured values, at least on a daily basis, with some under- or over-estimations depending on both the considered model and the particular sky conditions.

In the subsequent paper[1], we will review the best known methods for producing estimates of the solar global irradiance at ground level which use suitable physical models of the atmosphere; the paper will also draw more general conclusions.

Acknowledgments—The comments and suggestions by Dr. A. Zelenka, Swiss Meteorological Institute, Zürich, were greatly appreciated.

NOMENCLATURE

- A surface albedo of the earth
- B brightness, i.e., digital counts measured by the satellite, proportional to the upward solar radiation emerging from the atmosphere
- B_{cld} mean cloud brightness (T)
- B_m mean target brightness, i.e., mean brightness of a pixel array (T and JPT)
- B_{max} maximum brightness, giving information on the cloud albedo (T)
- B_{max} threshold brightness (JPT)
- B_{min} threshold brightness (JPT)
- B_n normalized clear sky brightness, i.e., B_0 ($\theta = 45°$, $\phi = 105°$) (T)
- B_0 clear sky brightness (minimum brightness or clear brightness) (T)
- B'_0 observed clear sky brightness (JPT)
- E_A solar radiation absorbed by atmosphere
- E_G solar radiation absorbed by ground
- F_{cs} solar constant
- F_0 hourly value for the solar constant (JPT)
- HG hourly downward solar radiation incident on the earth surface, J m^{-2}
- $HE_\downarrow$ hourly downward solar radiation incident at the top of the atmosphere (C), J m^{-2}
- $IE_\uparrow$ flux density of the upward solar radiation emerging from the atmosphere and received by the satellite, W m^{-2}
- $IE_\downarrow$ flux density of the downward solar radiation incident on the atmosphere, W m^{-2}
- IG flux density of the downward solar radiation incident on the earth's surface, W m^{-2}
- m optical air mass
- n cloud cover index ($0 \le n \le 1$)
- n^t cloud cover indices at a time t (C)
- N total number of pixels in a target area (T)
- N_1 number of pixels in a target area in clear category (T)
- N_2 number of pixels in a target area in partly cloudy category (T)
- N_3 number of pixels in a target area in cloudy category (T)

r actual sun-earth distance
r_0 mean sun-earth distance
T shortwave atmospheric transmittance (HH)
T_r visible transmission due to Rayleigh scattering (T)
T' atmospheric transmittance for descending solar radiation, i.e., $\frac{IG}{IE_\downarrow}$, at time t(C)
T_{wa} visible transmission due to water vapor absorption (T)
T_{ws} visible transmission due to water vapor scattering (T), i.e., $\frac{IE_\uparrow}{A \times IG}$
$T(\theta)$ atmospheric transmittance for descending solar radiation, i.e., $\frac{IG}{IE_\downarrow}$
w precipitable water (T), cm
ϕ satellite zenith angle
θ solar zenith angle
θ_s satellite zenith angle (C)
ρ' reference albedo, i.e., $\frac{IE_\uparrow}{IG_0}$, at time t(C)
ρ_c average reference albedo of the cloud tops (C)
ρ_0 reference albedo in clear sky conditions (C)

REFERENCES

1. M. Noia, C. F. Ratto, and R. Festa, Solar irradiance estimation from geostationary satellite data: II. Physical models, *Solar Energy* **51,** 457–465 (1993).
2. F. De Carli, C. Groppi, R. Festa, and C. F. Ratto, A procedure to obtain global radion maps from sunshine durations at isolated stations in a region with complex orography, *Solar Energy,* **37,** 91–108 (1986).
3. R. Festa and C. F. Ratto, Mapping the climate. In: R. Guzzi and C. G. Justus (eds.), *Physical climatology for solar and wind energy,* Lectures given at the International Centre for Theoretical Physics, 21 April–16 May 1986, Trieste, World Scientific Publishing Co., pp. 987–1060 (1988).
4. A. Zelenka, Satellite versus ground observation based model for global irradiation. In: K. G. T. Hollands and E. Bilgen (eds.), *INTERSOL* 85, *Proc. of Biennial Congress ISES,* Pergamon Press, Tarrytown, NY, pp. 2513–2517 (1986).
5. A. Zelenka, D. Lazic, and O. Jaquet, Solar resource assessment with geostatistical tools. In: *Clean and safe energy forever, Proc. of Biennial Congress ISES, Kobe,* 1990, Pergamon Press, Tarrytown, NY (1990).
6. V. D'Agostino and A. Zelenka, Supplementing radiation network data by cokriging with satellite images. In: *The Second CODATA Conference on Geomathematics and Geostatics* (1990).
7. U.S. Department of Commerce, *Studies of Cloud and Satellite Parametrization of Solar Radiation at the Earth's Surface, Proceedings of the Miami Conference on Remote Sensing* (1971).
8. T. H. Vonder Haar, Solar insolation microclimate determined using satellite data. In: *Solar Energy Data Workshop NOAA* (1973).
9. T. H. Vonder Haar and J. S. Ellis, Solar energy microclimate as determined from satellite observations, *Optics in Solar Energy Utilization* **68,** 18–28 (1975).
10. J. S. Ellis and T. H. Vonder Haar, Solar radiation reaching the ground determined from meteorological satellite data, Technical Report NTIS N79-27770/3GA, NASA (1979).
11. J. E. Hay and K. J. Hanson, A satellite-based methodology for determining solar irradiance at the ocean surface during GATE, *Bull. American Meteorol. Soc.* **59,** 1549 (1978).
12. J. D. Tarpley, Estimating incident solar radiation at the surface, from geostationary satellite data, *J. Appl. Meteorol.,* pp. 1172–1181 (1979).
13. C. Justus, M. V. Paris, and J. D. Tarpley, Satellite-measured insolation in the United States, Mexico, and South America, *Remote Sensing of Environment* **20,** 57–83 (1986).
14. D. Cano, J. M. Monget, M. Albuisson, H. Guillard, N. Regas, and L. Wald, A method for the determination of the global solar radiation from meteorological satellite data, *Solar Energy* **37,** 31–39 (1986).
15. C. Raphael, Models for estimating solar irradiance at the Earth's surface from satellite data: An initial assessment, Technical Report, Atmospheric Environment Service, Downsview Ontario (1983). (Unpublished manuscript.)
16. C. Raphael and J. E. Hay, An assessment of models which use satellite data to estimate solar irradiance at the Earth's surface, *J. Clim. App. Meteor.* **23,** 832–844 (1984).
17. G. Czeplak, M. Noia, and C. F. Ratto, An assessment of a statistical method to estimate solar irradiance at the Earth's surface from geostationary satellite data, *Renewable Energy* **1,** 737–743 (1992).
18. A. Zelenka *et al.,* Techniques for supplementing solar radiation Network data, Technical Report, International Energy Agency, # IEA-SHCP-9D-1, Swiss Meteorological Institute, Krahbuhlstr. 58, CH-8044 Zurich, Switzerland (1992).
19. S. Marullo, G. Dalu, and A. Viola, Incident short-wave radiation at the surface from meteosat data, *Il Nuovo Cimento* **10C,** 77–90 (1987).
20. C. Gautier, G. Diak, and S. Masse, A simple physical model to estimate incident solar radiation at the surface from GOES satellite data, *J. Appl. Meteorol.* **36** (1980).
21. W. E. Shenk and V. V. Salomonson, A simulation study exploring the effects of sensor spatial resolution on estimates of cloud cover from satellite, *J. Appl. Meteorol.* **11,** 214–220 (1972).
22. J. A. Davies, W. Schertzer, and M. Nunez, Estimating global solar radiation, *Boundary Layer Meteorology* **9,** 33–52 (1975).
23. J. E. Mc Donald, Direct absorption of solar radiation by atmospheric water vapour, *J. Meteorol.* **17,** 319–328 (1960).
24. D. Cano, Etude de l'Ennuagement par Analyse de Séquences d'Images de Satellite. Application à l'Evaluation du Rayonnement Solaire Gloibal au Sol, Ph.D. thesis, Ecole Nationale Supérieure des télécommunications (1982).
25. L. Diabaté, H. Demarcq, N. Michaud-Regas, and L. Wald, Estimating incident solar radiation at the surface from images of the Earth transmitted by geostationary satellites: The Heliosat project. *Int. J. Solar Energy* **5,** 261–278 (1988).
26. G. Moussu, L. Diabaté, and L. Wald, A method for the mapping of the apparent ground albedo brightness using visible images from geostationary satellites, *Remote Sensing of Environment* (1988).
27. L. Diabaté, G. Moussu, and L. Wald, Description of an operational tool for determining global solar radiation at ground using geostationary satellite images, *Solar Energy* **42,** 201–207 (1989).
28. G. Bourges, Courbes de Frequence Cumulees de l'Irradiation Solaire Globale Horaire Recue par une Surface Plane, Technical Report, Centre d'Energetique de l'Ecole National Superieur des Mines de Paris (July 1979).